



On the modern deep learning approaches for precipitation downscaling

Bipin Kumar¹ · Kaustubh Atey² · Bhupendra Bahadur Singh¹ · Rajib Chattpadhyay^{1,3} · Nachiketa Acharya^{4,5} · Manmeet Singh¹ · Ravi S. Nanjundiah⁶ · Suryachandra A. Rao¹

Received: 28 May 2022 / Accepted: 13 February 2023 / Published online: 3 March 2023
© The Author(s), under exclusive licence to Springer-Verlag GmbH Germany, part of Springer Nature 2023

Abstract

Deep Learning (DL) based downscaling has recently become a popular tool in earth sciences. Multiple DL methods are routinely used to downscale coarse-scale precipitation data to produce more accurate and reliable estimates at local scales. Several studies have used dynamical or statistical downscaling of precipitation, but the availability of ground truth still hinders the accuracy assessment. A key challenge to measuring such a method's accuracy is comparing the downscaled data to point-scale observations, which are often unavailable at such small scales. In this work, we carry out DL-based downscaling to estimate the local precipitation using gridded data from the India Meteorological Department (IMD). To test the efficacy of different DL approaches, we apply SR-GAN and three other contemporary approaches (viz., DeepSD, ConvLSTM, and UNET) for downscaling and evaluating their performance. The downscaled data is validated with precipitation values at IMD ground stations. We find overall reasonably well reproduction of original data in SR-GAN approach as noted through M.S.E., variance statistics and correlation coefficient (CC). It is found that the SR-GAN method outperforms three other methods documented in this work ($CC_{SR\text{-}GAN}=0.8806$; $CC_{UNET}=0.8399$; $CC_{CONVLSTM}=0.8311$; $CC_{DEEPS}=0.8037$). A custom V.G.G. network, used in the SR-GAN, is developed in this work using precipitation data. This DL method offers a promising alternative to other existing statistical downscaling approaches. It is noted that superiority in the SR-GAN approach is achieved through the perceptual loss concept, wherein it overcomes the issue of smooth reconstruction and is consequently able to capture better fine-scale details of data considered.

Keywords DL-based downscaling · V.G.G. model · SR-GAN · Station data · Kriging method · Climatology

Communicated by: H. Babaie

✉ Bipin Kumar
bipink@tropmet.res.in

¹ Indian Institute of Tropical Meteorology, Ministry of Earth Sciences, Government of India, Dr. Homi Bhabha Road, Pashan, Pune, India 411008

² Indian Institute of Science Education and Research, Dr. Homi Bhabha Road, Pashan, Pune 411008, India

³ Indian Meteorological Department, Ministry of Earth Sciences, Government of India, Shivaji Nagar, Pune 411005, India

⁴ Cooperative Institute for Research in Environmental Sciences (CIRES), University of Colorado Boulder, Boulder, CO, USA

⁵ National Oceanic and Atmospheric Administration (NOAA) Physical Sciences Laboratory, Boulder, CO, USA

⁶ Centre for Atmospheric & Oceanic Sciences and Divecha Centre for Climate Change, Indian Institute of Science, Bengaluru, India 560012

Introduction

There is an increasing demand for trustworthy weather and climate information at local sizes for improved management and preparedness of billions of people worldwide. The observational data (especially ground-based observations) lack the spatial resolution required to project meteorological information on a micro-scale describing features within cities or villages. Similarly, the outputs from global models (G.C.M.s/ESMs, etc.) are often coarse. They are less helpful in understanding the local weather and climate and the impacts on specific sectors, e.g., agriculture, food, water, etc. Precipitation is one such variable that can primarily affect these sectors. There is a requirement for developing more accurate rainfall datasets at finer scales, especially over Indian landmass, as documented in (Haq 2022a). Although India Meteorological Department (IMD) has good coverage of stations, the best available gridded data is still only

available at $0.25^\circ \times 0.25^\circ$ resolution. A long-pending question in this context is whether we can go for even higher-resolution gridded data reconstruction using the available station observations. To cater to such demands for high-resolution weather and climate data, forecasts and projections are being produced using state-of-the-art, statistical and deep learning (DL) models (Dueben and Bauer 2018; Kumar et al. 2021; Reichstein et al. 2019; Singh et al. 2021). These datasets are produced through a combination of different methods, each having its assumptions, advantages, and disadvantages. The methodology to obtain high-resolution weather and climate information assumes that the local climate results from interactions between large-scale atmospheric characteristics (circulation, temperature, moisture, etc.) and local features (topography, water bodies, land use—land cover, etc.). One of the most popular techniques to derive weather and climate information at finer scales is done through downscaling. Downscaling is a technique for adding additional high-resolution information to coarse datasets to obtain more reliable data at a finer spatial scale, better capturing regional gradients and local inhomogeneities.

Although the information can be downscaled on both spatial and temporal dimensions, often, it is the spatial information that is sought after in the weather and climate science and allied sectors. Regional models utilize the outputs from global models to produce dynamical downscaling by taking the large-scale atmospheric and oceanic conditions at the lateral boundaries (Sanjay et al. 2020). These models incorporate complex topography, the land-sea contrast, surface heterogeneities, and detailed descriptions of physical processes to generate realistic climate information at regional scales. A key limitation of this approach is its reliance on the accuracy of global model fields and inherent biases (Seaby et al. 2013). Thus, it requires a bias correction before going for further downscaling.

Furthermore, the precipitation product is often erroneous in global and regional models. The observation data are generally downscaled using different interpolation techniques (Pai et al. 2014; Rajeevan et al. 2006). This issue can be addressed further using an alternative approach known as Statistical Downscaling (S.D.) (Baño-Medina et al., 2020), which involves the establishment of an empirical relationship between historical/processed data (such as station data to the grid) and real-time/observational data (such as weather station data to the grid). Here, we explore the feasibility and reliability of generating high-resolution gridded data from DL techniques and ground observations. One such technique is the deep neural network, widely used in a variety of areas, including error detection in IoT, Botnet detection (Haq et al., 2022; Haq and Khan 2022), and in forecasting and analyzing the meteorological variables (Haq 2022a, 2022b; Kumar et al. 2022).

DL-based downscaling is one type of S.D. that can be achieved using a variety of methods. The DL methods are

beneficial for generating high-resolution images for given low-resolution inputs. It has been used widely by the computer vision community. Researchers have used the same concept by considering the meteorological data (the precipitation data in this case) as an image to generate a downscaled precipitation map. Deep Statistical Downscaling (DeepSD) was one of the first works that attempted the downscaling problem using DL techniques (Vandal et al. 2017). It used an SRCNN network (Dong et al. 2015) and leveraged topography/ elevation with low-resolution precipitation data as input. The high-resolution topographical features aid in learning to estimate spatial precipitation patterns in high resolution. Kumar et al. (2021) used DeepSD for downscaling precipitation data over the Indian region. This work showed that DeepSD successfully outperformed other methods like linear interpolation, Super Resolution Convolutional Neural Networks (SRCNN), and stacked SRCNN. Augmented Convolutional Long Short Term Memory (ConvLSTM) is another technique that uses a recurrent convolutional LSTM approach for downscaling climate data (Harilal et al. 2021). This work captured both temporal and spatial dependencies using the ConvLSTM layers. On top of the recurrent layers, they used a novel super-resolution block that increased the spatial resolution of high-dimensional features obtained from the preceding ConvLSTM layers. In addition to the precipitation and elevation, the input was augmented with other physics-guided auxiliary variables like relative humidity, pressure, and wind components. Capturing spatiotemporal dependencies and including additional input variables allowed this method to outperform downscaling methods like ResLap (Cheng et al. 2020) and DeepSD. It is to be noted that DeepSD and Augmented ConvLSTM use Mean Squared Error (M.S.E.) and Root Mean Squared Error (RMSE) as loss functions, respectively. A significant drawback of using such loss functions is that the generated solution appears overly smooth due to the point-wise average of the solutions. As a result, the reconstructions fail to capture finer spatial patterns. The researchers (Passarella et al. 2022) present a method called Fast Super-Resolution Convolutional Neural Network (FSRCNN) based approach for downscaling earth system model (ESM). Serifi et al. (2021) presented Deconvolutional (D.C.N.) U-Net, an encoder-decoder architecture for precipitation downscaling. This method combined the L1 norm with gradient loss as a loss function to address the smooth reconstruction problem. Penalizing for the gradient differences allowed the reconstruction of higher-frequency details.

The Generative Adversarial Network (GAN), another approach (Goodfellow et al. 2014) to produce a high-resolution image from a low-resolution input, describes uncertainty using contemporary machine-learning techniques primarily independent of any specific statistical assumption (Gagne et al. 2020). This approach has also been applied recently to the time evolution of atmospheric variables (Leinonen et al.

2020). Several versions of GAN approaches are presently being explored across the domains. The stochastic super-resolution GAN (Leinonen et al. 2019) provides an ensemble of plausible high-resolution outputs for a given input. This GAN method has been widely used for meteorological data downscaling (Harris et al. 2022; Liu et al. 2022; Stengel et al. 2020). The other potential method for downscaling the meteorological data is the Super-resolution Generative Adversarial Network (SR-GAN) method proposed by Ledig et al. (2017). The SR-GAN primarily aims to improve the perceptual quality of the reconstructed image on resolution enhancement. More details of this method are provided in "Methods".

Despite several studies adopting dynamical or statistical downscaling of precipitation, the statement on accuracy is limited by the availability of ground truth. The main challenge lies in determining whether the downscaled gridded data can be matched to point-scale observations. Modern techniques frequently fall short, and the problem of obtaining local precipitation information becomes stalled as there is not enough information to provide a reliable estimate of accuracy. Here, we carry out the DL-based downscaling to estimate the local projection of precipitation data available from the IMD, created by approximating the value from station location to grid point. We apply four approaches to evaluate their performance and present the analysis results through robust statistical estimates. The considered approaches are DeepSD, ConvLSTM, U-NET, and SR-GAN. This study's primary objective is to document the performance of a few state-of-the-art DL methods, as discussed earlier, for precipitation downscaling. It is shown here that SR-GAN outperforms other existing algorithms for the particular data utilized in this study. The literature considers the SR-GAN a promising method for meteorological data downscaling. The novelty in this method is developing a customized model (based on an existing V.G.G. library) that was trained on precipitation data.

The paper is organized as follows. The downscaling methods used in this work are detailed in "Methods" (methodology), followed by the data pre-processing procedure in "Data pre-processing and training". Results are presented in "Results", and "Conclusion and discussion" provides the conclusion and discussions on this work. Figure 1 illustrates a birds-eye view of the work done in this manuscript. We used the SR-GAN model (the best one among the four models used) to downscale the IMD gridded data up to $4 \times$ resolution and validate it with ground station observations.

Methods

A statistical downscaling (S.D.) can be formulated as a functional mapping between low-resolution (L.R.) data and corresponding high-resolution (H.R.) data. An S.D.

model takes X: L.R. data as input and generates \hat{Y} : the high-resolution data as output

$$\hat{Y} = F(\Theta, X) \quad (1)$$

The objective is to find a set of parameters (Θ) such as the loss $L(Y, \hat{Y})$ between the generated and the ground truth data (Y) is minimized. Several methods are available in the literature for statistical downscaling described in the previous section.

As discussed in the introduction section, the GAN-based algorithm, called SR-GAN, proposed by (Ledig et al. 2017), is more successful in generating the super-resolution of a single picture than the previous one. It uses a novel perceptual loss to address the smooth reconstruction problem. When dealing with colossal scaling factors, it is still possible to retrieve the finer elements of the original image (Xiong et al. 2020). The adversarial component (refer to Fig. 3) of the perceptual loss drives the reconstruction solution toward natural-looking image space with high perceptual quality. This algorithm has been used for single-picture super-resolution tasks (Izumi et al. 2022) and for generating high-resolution multi-regional climate data by Norihiro Oyama et al. (2022). They proposed a method called π -SR-GAN (Physics Informed Super-Resolution Generative Adversarial Network).

The SR-GAN method has been employed in this work, and its performance is compared to that of three other algorithms (DeepSD, ConvLSTM, and U-NET) used for ML-based data downscaling.

Table 1 shows the architecture of all four models. These models were trained on the L.R. (1°) IMD data for $4 \times$ resolution enhancement, and we compared the results using correlation as a metric. Deep learning algorithms for data downscaling are frequently used with a loss function based on the M.S.E. (Kumar et al. 2021; Harilal et al. 2021). Due to the point-wise average of the solutions, one of the most significant disadvantages of utilizing an MSE-based loss function is that the resulting solution seems excessively smooth. SR-GAN solves this problem by employing a unique loss function known as perceptual loss, which is helpful in adversarial training situations. Also, it helps to recover the final details of the data. When calculating the perceptual loss, Ledig et al. (2017) use a weighted sum of content and adversarial loss content, as shown in Eq. 2 below.

$$l^{SR} = \underbrace{l_X^{SR}}_{contentloss} + 10^{-3} \underbrace{l_{Gen}^{SR}}_{adversarialloss} \quad (2)$$

Equation 2, has been used in this study to train the V.G.G. network using precipitation data; more details of this network have been provided in "Data pre-processing".

Fig. 1 Schematic of the work-plan carried out in this study to generate and compare high-resolution downscaled precipitation data

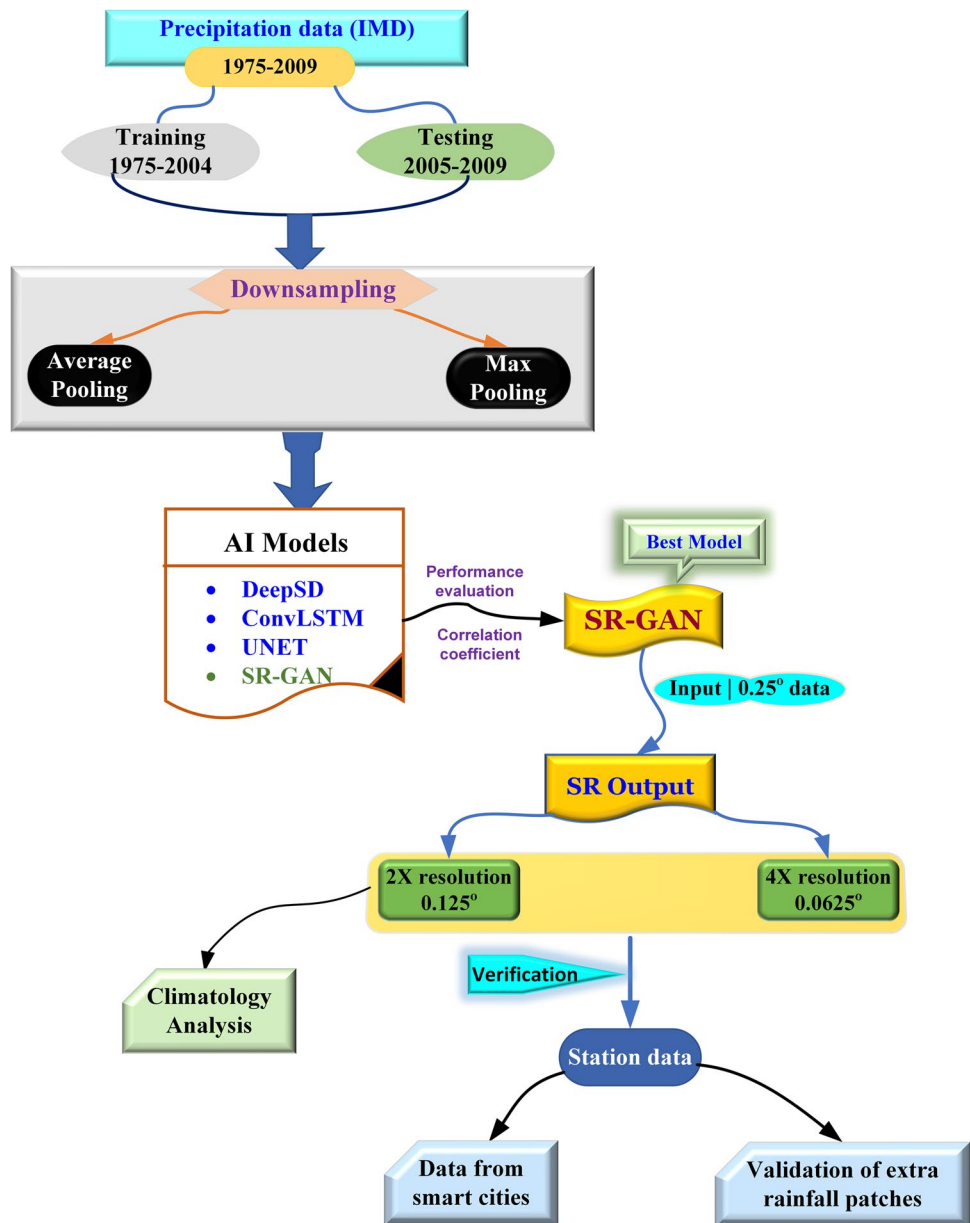


Table 1 List of hyperparameters used in the four models. The Adaptive Moment Estimation (ADAM) optimizer was used in all models, which provided faster convergence

Model	Activation function	Learning rate	Loss function	Batch size
DeepSD	PRELU (Parametric Rectified Linear Unit)	0.001	MSE	200
Augmented ConvLSTM	Conv-2D- RELU	0.0003	RMSE	8
UNET	Conv-2D- RELU	0.001	Grad Loss (Custom)	8
SR-GAN	Generator- Residual Blocks – PRELU Generator- UpSampling Blocks- PRELU Discriminator- Conv Body- Leaky RELU Discriminator- Dense 1- Leaky RELU Discriminator-k Dense 2- Sigmoid	0.0001	Perceptual Loss (Custom)	256

The Kriging method

In this study, the downscaled data obtained from the DL method has been verified from actual station data by approximating the precipitation values at the grid point to the nearest station. The kriging method (Oliver and Webster 1990) interpolates the precipitation values at grid points to station locations. According to Haq et al. (2021), the kriging approach is believed to be superior than the other methods. The kriging approach uses statistical correlations among the observed points to generate the values. For a given grid point, $u_{i,j}$, a function f to approximate the value from grid point to station location can be written as

$$f(x, y, z) = \frac{\sum_{i=0}^n w_i u_i}{\sum_{i=1}^n w_i} \quad (3)$$

where (x, y) are latitude and longitude, and 'z' represents the elevation of a particular grid point, 'n' is the total number of grid points in a specified radius (see Fig. 8). The weights w_i are determined in terms of the distance 'd' between the station location and the grid point. Now consider a vector $u_0 = uw^T$, w is the weight vector calculated as $Aw = b$, where,

$$A = r(x_i, x_j), b = r(x_0, x_i) \text{ and } r = \frac{1}{2}(u(x+h) - u(x))^2 \quad (4)$$

Here, x_0 represents the location of the point of interest, and the respective precipitation value is u_0 . Then the approximation function (Eq. 3) can be written as

$$\hat{f} = uw^T \quad (5)$$

The grid values are approximated using Eq. 5.

Data pre-processing and training

Data description

The IMD gridded data (Pai et al. 2014; Rajeevan et al. 2006) was used for training in this study. This data is available in two resolutions: ($1^\circ \times 1^\circ \sim 110 \text{ km} \times 110 \text{ km}$) and ($0.25^\circ \times 0.25^\circ \sim 25 \text{ km} \times 25 \text{ km}$). The 1° data has dimensions of (33,33) and 0.25 (129,135).

The details of the time duration for the data are provided in Table 2.

In addition to the IMD gridded data, we have considered the IMD station data over time (2005–2009) to validate the DL model output. The specifics of the stations from which the data was gathered are provided in "Validating the high-resolution output with station data".

Data pre-processing

We have mainly used the 0.25° data, which was downsampled (coarse resolution) to 1° data. This process was carried out because of the non-similarity in both data. In particular, the low-resolution data was prepared using fewer ground stations available at that time. Gradually, the number of stations in 2014 increased, and the high-resolution data was prepared using more ground stations. The downsampling was carried out using the following two steps.

- (1) Average pooling with (2,2) kernel
- (2) Max pooling with (2,2) kernel.

The minimum and maximum precipitation values are calculated by grouping the same days for all the years, and min–max normalization is employed to scale data in the range of [0,1]. The formula used for normalization is $Z = \frac{X - X_{min}}{X_{max} - X_{min}}$

V.G.G. training for precipitation data

As mentioned in "Methods", the SR-GAN method uses a unique loss function called perceptual loss, which has two components: content loss and adversarial loss. The content loss (Eq. 6), also known as the V.G.G. (Visual Geometry Group) Loss, is defined as the Euclidean distance between the feature representations of the produced data \hat{Y} and the corresponding ground truth data (Y). The V.G.G. network (Simonyan and Zisserman 2015) was developed by a group at the University of Oxford (<https://www.robots.ox.ac.uk/~vgg/>). The data is fed into a pre-trained V.G.G. network, which produces feature representations. The content/V.G.G. loss is defined as (Ledig et al. 2017)

$$l_{VGG/i,j}^{SR} = \frac{1}{W_{i,j}H_{i,j}} \sum_{x=1}^{W_{i,j}} \sum_{y=1}^{H_{i,j}} \left(\phi_{i,j}(Y)_{x,y} - \phi_{i,j}(G(\hat{Y}))_{x,y,i,j} \right)^2 \quad (6)$$

Here $W_{i,j}$ and $H_{i,j}$ are the dimension of the respective feature map within the V.G.G. network. The $\phi_{i,j}$ are the feature extraction map and Y and \hat{Y} are the target and predicted data (generated from SR-GAN), respectively, and G is a generator function that estimates lower resolution images to higher-resolution ones. Because they were trained on the ImageNet dataset, which consists of natural RGB images, we could not use the publicly available pre-trained V.G.G. networks in this study because those did not produce good results. Instead, we trained a V.G.G. network on meteorological data in such a way that

Table 2 Details of the IMD gridded data used for training and testing (also referred to as ground truth (G.T.) data)

	Data	Training	Testing
IMD	1975–2004	2005–2009	

it learns a rich feature representation for meteorological variables through experimentation. Thus, we developed a novel V.G.G. model that works on meteorological data. A sketch illustrating the training architecture is provided in Fig. 2. During SR-GAN adversarial training, this trained model computes the content loss component of perceptual loss. We used the same data for the V.G.G. training, which was used for model training, i.e., for the duration 1975–2004. It contains many layers to extract finer scale features, as depicted in Fig. 1; more details can be found in (Simonyan and Zisserman 2015). Figure 3 presents an overview of the SR-GAN flow used in this work. It depicts the role of the V.G.G. model. It calculates the perceptual loss to evaluate the output image produced by the generator model; it works as the interface between the generator and discriminator part of the model.

Other aspects of training

The SR-GAN method contains two networks, namely, generator and discriminator networks. Firstly, the generator network is initialized by pre-training using an M.S.E. loss function. Such initialization enables the generator to avoid undesired local optima during adversarial training. Finally, the pre-trained generator is trained alongside the discriminator network in an adversarial setting using perceptual loss. The discriminator learns to differentiate between the generated output (S.R.) and the ground truth (G.T.). The V.G.G. and discriminator feedback are used to calculate the perceptual loss. Backpropagation of the perceptual loss to the generator allows it to generate finer texture details. The details of all three training are provided in Table 3.

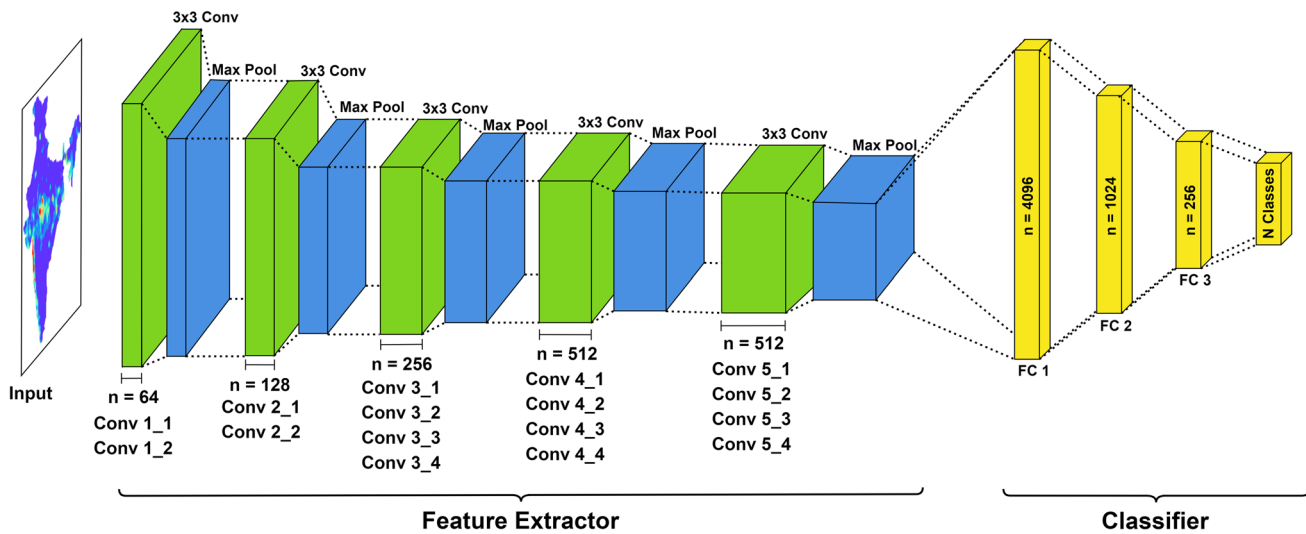


Fig. 2 The details of the VGG training architecture used for precipitation data

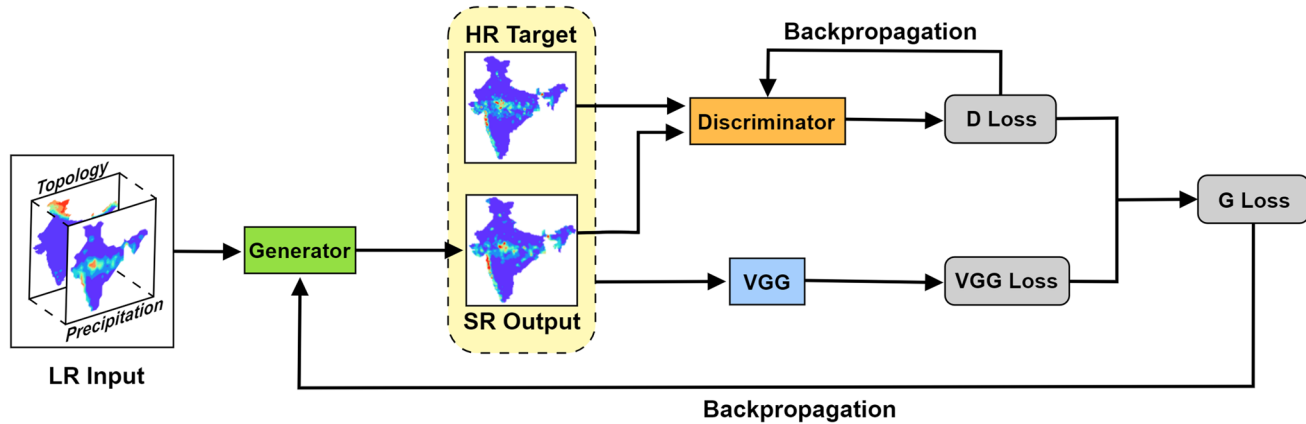


Fig. 3 Description of the SR-GAN model indicating the role of the pre-trained V.G.G. model in calculating the perceptual or V.G.G. loss

We have developed a custom-trained V.G.G. network for precipitation data. We built on the original VGG-19 architecture (cite), keeping the feature extraction layers the same and modifying the classifier layers, as depicted in Fig. 2. In the classifier network, we alter the number of neurons in each layer and append an additional dense layer to it.

We experiment with the number of residual blocks in the generator architecture to study the effect on the model's performance. Here the number of residual blocks was: reduced by a factor of two (i.e., 8), increased by a factor of two (i.e., 32), and kept constant as the original work (i.e., 16) to assess the configuration that works best for our use case. We noticed that using eight residual blocks yields the best results for our use case. A probable reason for this can be that even after using skip connections, the features get diminished in deeper layers. Also, as our data is not very big, using a too-deep network may not suit our task. Another benefit of using eight residual blocks is faster training and convergence. The SR-GAN model integrated with the newly developed pre-trained V.G.G. model has been used in this work for the local projections of the IMD gridded data.

Results

We utilized IMD gridded data, as stated in the previous section. We applied four DL-based downscaling algorithms to this data, described in "Methods". The provided data has

been pre-processed using the methods listed above. Figure 4 depicts a representative data snapshot in both low and high resolution.

The resulting downscaled data (1° to 0.25°) was compared to available H.R. (0.25°) data. An illustration of the comparison of correlation PDFs (Probability Density Functions) obtained using these four approaches is shown in Fig. 5. As can be seen, the SR-GAN appeared to be the most effective approach in correlation coefficient comparison. Our custom pre-trained V.G.G. feature extractor led the SR-GAN model to generate and recover higher frequency details. The correlation PDF comparison confirms that SR-GAN is one of the best methods for DL downscaling among the four methods discussed in this study. In the next step, we applied this method to generate high-resolution (up to $4 \times$ resolution) gridded data.

Generation of high-resolution data using IMD 0.25° data

We have determined that the SR-GAN method is the best among four methods: DeepSD, ConvLSTM, U-NET, and SR-GAN. This method has been used to generate the high-resolution IMD data, particularly from 0.25° , as input, to 0.125° (2x) and 0.0625° (4x) resolution.

The same (SR-GAN) model architecture has been used to create this high-resolution data. The dataset's duration

Table 3 Details of parameters used for training of different components of SR-GAN

Model	Optimizer	Loss function	Batch Size	Epochs
V.G.G	Adam (lr=10 -2)	Cross Entropy	512	100
Generator only	Adam (lr=10 -4)	Mean squared error	512	1000
Discriminator	Adam (lr=10 -5)	Perceptual Loss	256	1500

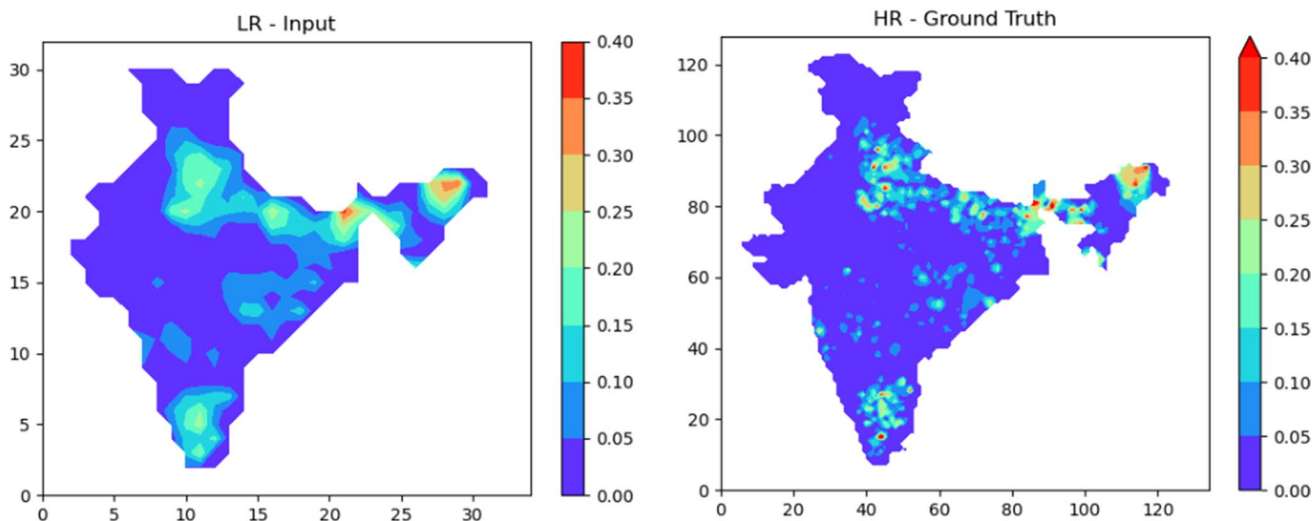


Fig. 4 A 2D representation of 1° (low resolution) input data (Left); 0.25° (high resolution) target data (Right)

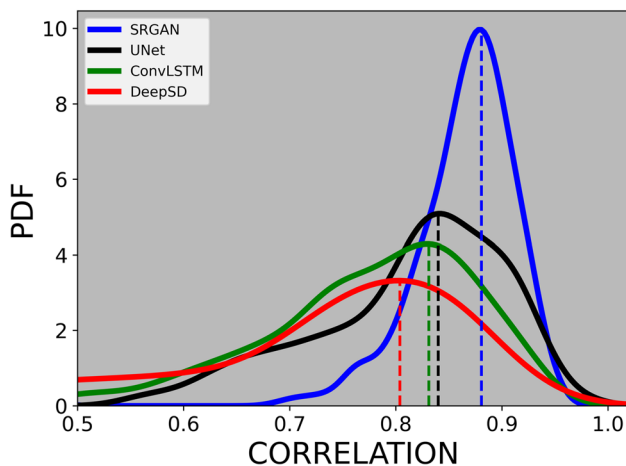


Fig. 5 Comparison of correlation obtained using HR data and resulting data from the four methods for the time duration 2004–2009

also remains the same. Figure 6 visually compares rainfall data for a particular day, i.e., 5th August 2005. The outputted datasets show localized rainfall patches in both high-resolution data sets. We noted that these rainfall values were not present in the available IMD gridded data of $0.25^\circ \times 0.25^\circ$ resolution. In a later Section 4.3, we check the accuracy of these rainfall patches with observed station rainfall values.

Validating the high-resolution output with station data

The high-resolution IMD gridded data (0.125° and 0.0625°) obtained using the SR-GAN method (see Fig. 4) has been validated with rainfall values at the ground station. The validations for both resolutions were performed by interpolating the downscale data, using the Kriging method explained in "Methods", to the station locations as well as comparing the M.S.E. and correlation. We considered a few IMD ground observation stations located in the various smart

cities of India (<https://smartcities.gov.in/>). Although the government of India has named 100 cities as smart cities, IMD stations are present only in 78 cities. A total of 1040 IMD stations were found in these 78 smart cities. We used the actual precipitation values at stations from these cities to validate our high-resolution gridded data obtained from A.I. model output. First, a PDF of M.S.E. (between station data and interpolated downscale data of these ground stations) for 0.125° resolution data has been calculated and compared with variance in precipitation data for the duration (2004–2009). This comparison is presented in Fig. 7a. Further, a correlation PDF comparison obtained by the SR-GAN method and DeepSD, using the same data, is depicted in Fig. 7b. It shows that the SR-GAN method is better at capturing rainfall values.

Apart from comparing M.S.E. and correlation PDF, we have validated the data for a few selected cities by comparing the M.S.E. and variances in the data. Here, the city selection was done based on data availability and spread across different geographic locations of the country. For robust quantifications, we chose the cities so that each part has at least three stations or more. After obtaining the rainfall values on station location, we calculated the M.S.E. and compared this with variance in the data for several cities in central India, as depicted in Fig. 7c. A total of four cities were selected for the comparison in this panel, and in each case, the M.S.E. was found to be smaller than the variation.

Similarly, comparisons have been made for many other Indian towns in the northern, southern, western, and eastern regions. As can be observed in Fig. 7d–g, the M.S.E. has been consistently lower than the variance in virtually all situations. This analysis validates the correctness of the high-resolution data obtained from SR-GAN. After validating the $2 \times$ resolution data with station values, we generated the $4 \times$ resolution data, i.e., for 0.0625° , and did a similar analysis. In this data, again, we found the M.S.E. value lower than the data variance. The values of MSE PDF compared with variance PDF for the same stations

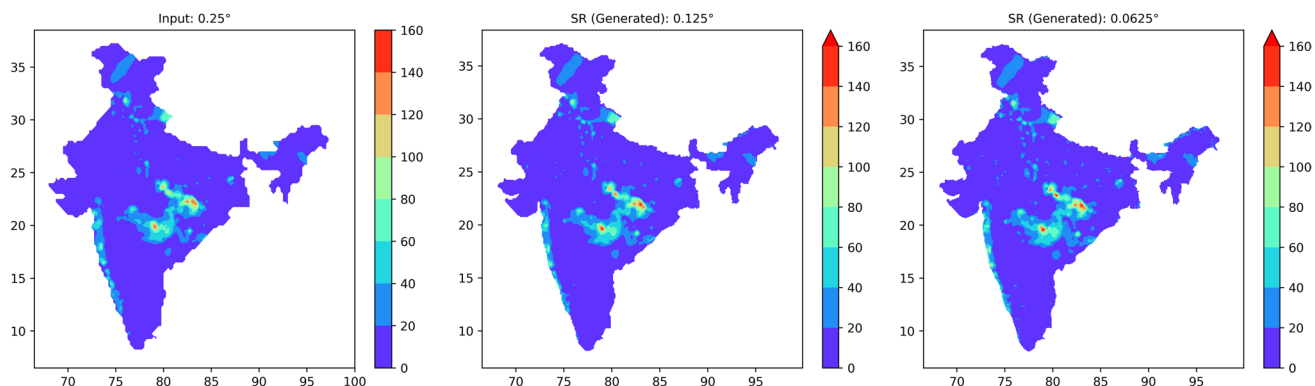


Fig. 6 Visual representation of rainfall data downscaling up to $4 \times$ resolution for the day 05-08-2005

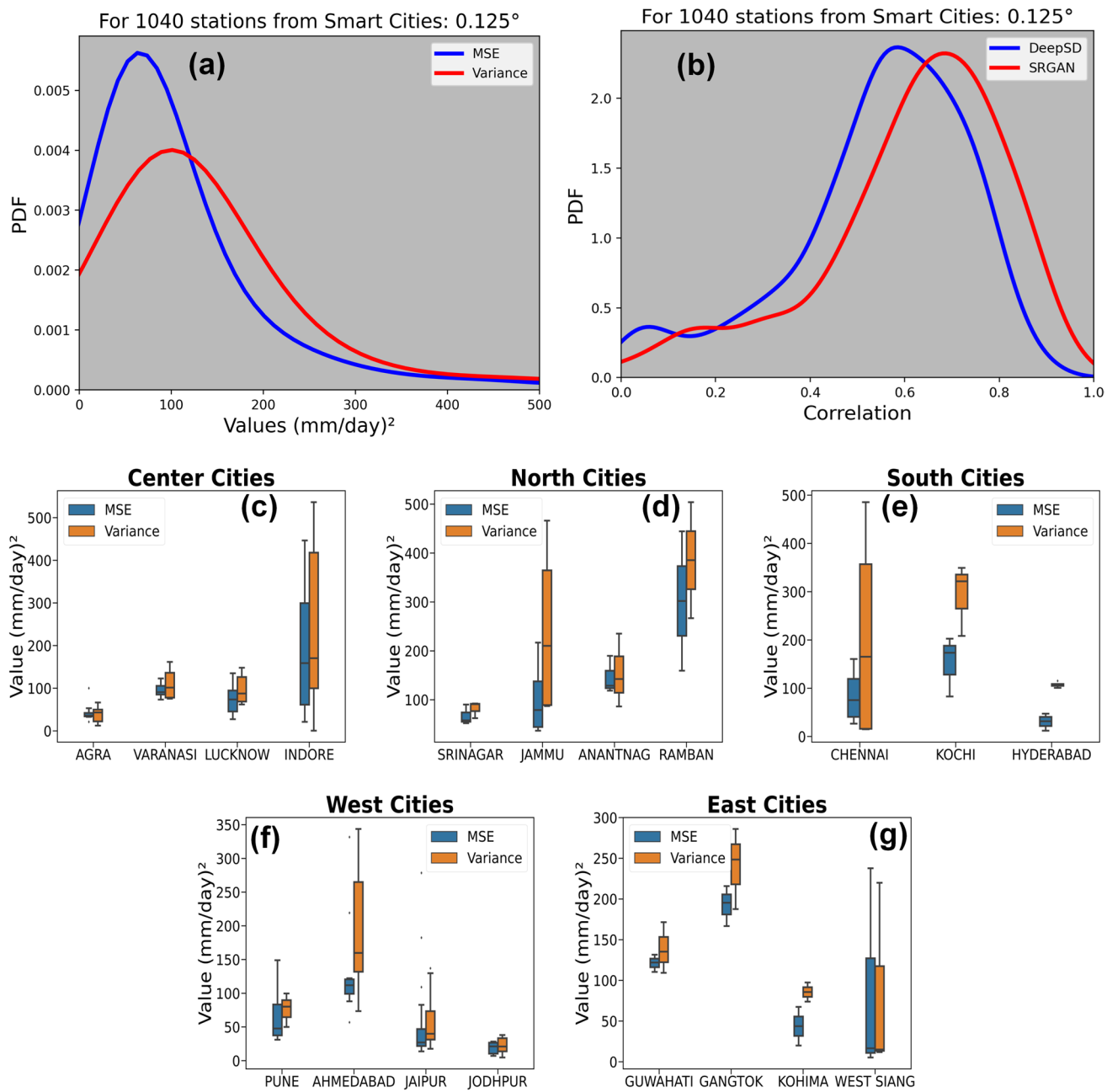


Fig. 7 Comparison of MSE and variance (panel **a**) for 1040 stations from 78 smart cities of India for the $2 \times$ high resolution, i.e., 0.125° data. Panel **(b)** depicts the correlation comparison obtained from

downscaled gridded data the station data of the same 1040 stations using SR-GAN and liner interpolation. A comparison of variance and MSE for selected cities are presented in the panels **(c)–(g)**

from the same number of smart Indian cities are presented in Fig. 8.

The analysis presented in Figs. 7 and 8 proved that the data obtained from the SR-GAN method is valid. The next step remains to validate the extra rainfall values that appeared at the new locations (which didn't exist in the original coarser grid) in the high-resolution map. The values at these locations have been compared with the nearest IMD station. This process is discussed in the next section.

Validating the additional information from ground stations

We did this comparison exercise to determine whether the model generated ‘false positives’ or it is reproducing the actual data. The 2D map of the high-resolution (0.125°) data, as depicted in Fig. 4, has additional grid points representing the rainfall values that are absent in the original data (see the first panel). To verify the legitimacy of additional rainfall

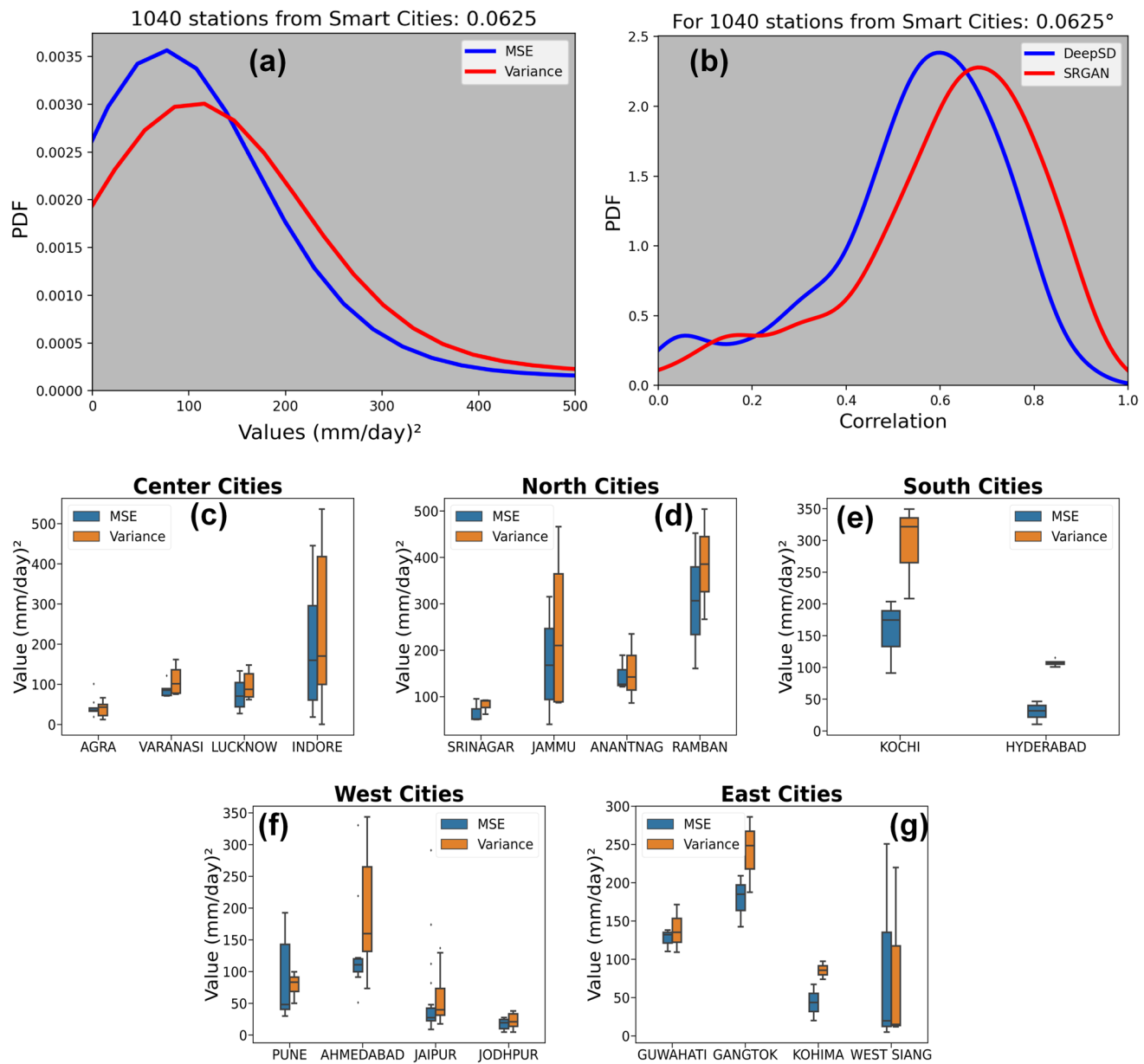


Fig. 8 Similar comparison as in Fig. 7 but for $4 \times$ resolution data (0.0625°) data

appearing on the finer grid, we collected the coordinates of those points, located the nearby stations, and compared the rainfall of those stations. Panel (B) of Fig. 7 indicates some additional rainfall patches obtained from the high-resolution data. Their zoomed locations (with Lat and Lon) are shown in panels (A, D, and E). These extra patches were validated with the actual rainfall values at nearby IMD ground stations.

First, the stations lying in a 12 km radius area were located then the precipitation values at grid points were approximated to the station location using the Kriging method described in "The Kriging method". The approximated values were compared to the actual observation rainfall values at that station.

Panel (f) of Fig. 9 depicted such a comparison of precipitation values on a particular day, 05-08-2005. It was found that the precipitation was recorded to those IMD stations on a specific day which was not present in the original gridded data of 0.25° resolution. Thus, the downscaling method was ideally validated with the actual observation.

Climatology analysis

Using the original data as input, $2 \times$ resolution, and $4 \times$ resolution data (obtained from the SR-GAN method), we calculated the climatology for the test data time duration

(i.e., 2005–2009). We compared it with the DeepSD model as a reference. The spatial plots for all three climatology datasets are depicted in Fig. 10 (panels a–c). They show that the small-scale spatial variations are visible in high-resolution data, while larger patterns are preserved in downscaled data. Furthermore, we calculated the biases in climatology using the original input data and DeepSD and SR-GAN generated data. The bias comparison in panels (d) and (e) show that the DeepSD model overestimates the climatology at almost all the locations. Even the actual precipitation values at the station's location are overestimated, as depicted in panel (f). Panels (g) & (h) bespeak that the precipitation climatology in the Western Ghats and North-East region is enhanced using SR-GAN generated high-resolution data.

Moreover, the precipitation values at station locations are close to the actual observation values (see panel (i)). DeepSD generally overestimates the rainfall by about 25%, whereas the SR-GAN estimates are closer, and the bias is further reduced by half. Thus, the SR-GAN is the best method for precipitation downscaling, as evidenced by climatological bias analysis.

Conclusion and discussion

An accurately downscaled climate data has several practical applications. Several statistical downscaling methods are available to generate such high-resolution data from low-resolution meteorological data. This study used different deep learning methods to downscale the gridded precipitation data available from IMD. We used low-resolution gridded precipitation data ($\sim 25 \text{ km} \times 25 \text{ km}$) as input to make $2x$ ($\sim 12 \text{ km} \times 12 \text{ km}$) and $4x$ ($\sim 6 \text{ km} \times 6 \text{ km}$) high-resolution data as output. Four deep-learning methods were used for this purpose. Previously published research by (Harilal et al. 2021; Kumar et al. 2021) employed two different methods (DeepSD and augmented ConvLSTM) to accomplish this objective, and we followed their lead. By comparing the correlation coefficients between these two investigations, Harilal et al. (2021) concluded that the augmented ConvLSTM approach outperformed the DeepSD method employed by Kumar et al. (2021). In this work, we built on the findings of the previous two studies and utilized two more approaches, namely U-NET and SR-GAN. Due to the point-wise average of the solutions, one of the

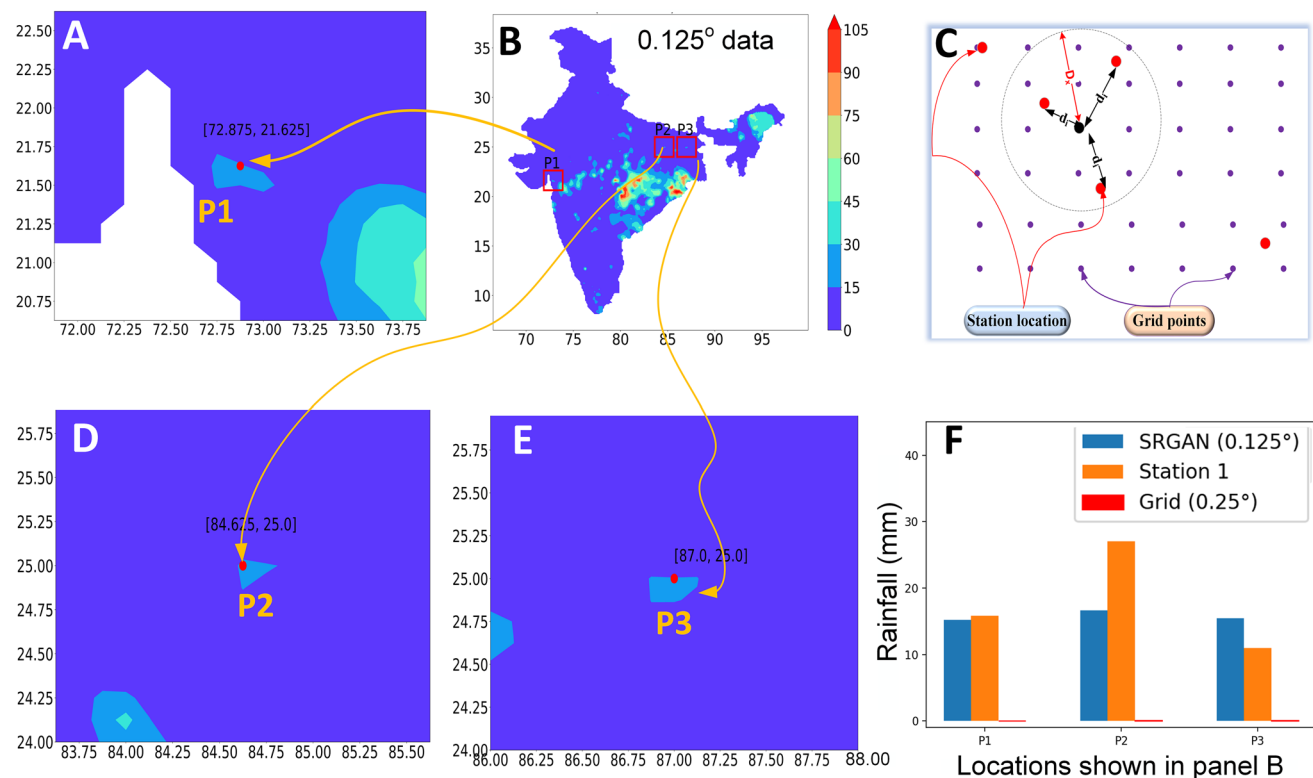


Fig. 9 Validating the extra points obtained from the SR-GAN method for high-resolution data. The additional rainfall points obtained are shown in panel (B). The zoomed versions of those points are represented in panels (A, D, and E). We used a search radius of 12 km to locate the nearest ground station, as depicted in panel (C). In this

panel, the blue dots represent grid points in gridded data, and the red dots represent the IMD station locations. Panel (F) compares the predicted rainfall values, and actual values recorded at the nearest stations

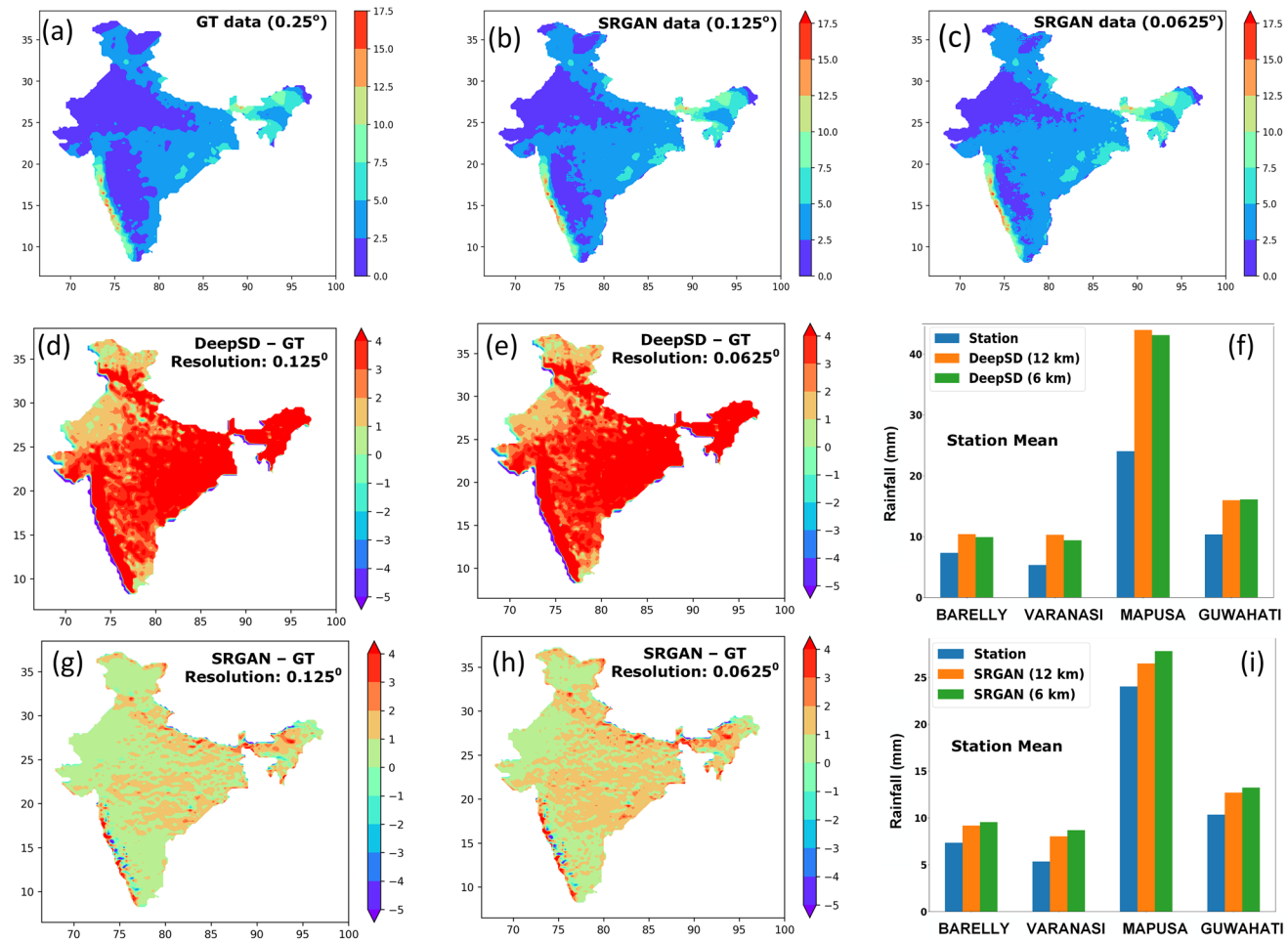


Fig. 10 The climatology analysis of down-scaled data. Panels **a–c** depict the climatology for test data (2005–2009) i.e. IMD gridded data (indicated as GT), SR-GAN (0.125°) and SR-GAN (0.0625°). Panels **d** and **e** represent climatological biases for 2× and 4× resolution data for DeepSD and the panel **f** compares the station mean

values with DeepSD generated values at those locations. Similarly, panels **g** and **h** have SR-GAN climatological biases and **i** is for comparison with SR-GAN generated mean values. These biases are calculated using original 0.25° data

most significant disadvantages of using an MSE-based loss function in DeepSD and ConvLSTM methods is that the resulting solution seems excessively smooth. The SR-GAN-based approach solves this problem by employing a unique loss function that captures spatial features better.

It was noted that the initial V.G.G. model used in the SR-GAN algorithm, given by the developer, was trained on an image collection and did not perform well on the precipitation data. In particular, the correlation value was relatively poor, and the fine details of precipitation values were not captured. Therefore, we constructed a unique V.G.G. model, which we trained using precipitation data to achieve our goals. With a customized V.G.G. model, and hence the perceptual loss function, the SR-GAN method captured fine-scale structure and outperformed the other three DL models used in this study. Particular attention was paid to the correlation coefficient metric, showing that SR-GAN and the

developed custom V.G.G. model are the most data-driven technique for statistical downscaling of precipitation data. Based on the correlation coefficient comparison, we concluded that the SR-GAN was the best DL model among the four models employed on the precipitation data. We utilized this approach and generated gridded data at a resolution of two and four times the original data.

In addition, we have shown some specific cases in which the SR-GAN method can enhance the rainfall amplitude (Fig. 9). We find that the enhancement in station rainfall amplitude through SR-GAN reduces the overall M.S.E. (Figs. 7 and 8). When comparing 2x-resolution data to low-resolution data, the 2x-resolution data contained additional points (refer to Figs. 6 and 9). We considered the precipitation values from a few nearby ground stations and compared them to the rainfall values at those stations to validate these additional points. To obtain the ground station

locations, we searched an area with a radius equal to or less than the grid size. For example, in the instance of 0.125° data (approximate 12.5 km grid resolution), we searched an area with a radius of 12 km to find the ground station locations, as shown in Fig. 7. Using the high-resolution data, we found precipitation values available at the locations of additional points were not present in the original low-resolution data. As a result, the high-resolution data has been validated using station values. We attempted to create data with a $4 \times$ resolution and obtained additional spots on the map. The new data has also been verified with the help of station data. We note that the M.S.E. of the high-resolution data is much lower than the data variance. The M.S.E. further reduces when we go to even higher-resolution data.

The climatological bias analysis (Fig. 10) suggests that the SR-GAN method has much fewer biases in the downscaled precipitation climatology than the DeepSD model. Station-based analysis suggests that DeepSD overestimates the rainfall climatology, which is corrected by SR-GAN-based model climatology. In particular, we found an increase in climatology for high-resolution data in the areas with high elevations, such as the Western Ghats and the North-East region of India. Thus, suitable downscaling is essential for the regions with orography and can improve the extreme event statistics for areas with elevated orography. This analysis can have several practical applications, e.g., verification of high-resolution model forecasts and district or block-level data generation for operational monitoring of rainfall during extreme events.

However, it is to be noted that further improvements can be made in the model architecture of both the generator and the discriminator networks of the SR-GAN method. Also, adding more inputs in the form of meteorological variables, e.g. temperature, humidity etc., apart from elevation and precipitation, can further lead to production of better quality precipitation data.

Acknowledgements IITM Pune is funded by the Ministry of Earth Science (MoES), the Government of India. This work was done using HPC facilities provided by MoES at IITM Pune.

Author contribution B.K., B.B.S., and R.C. have conceptualized the idea and contributed to the manuscript preparation. K.A. developed the code for the DL methods, analyzed the data and produced the plots. R.S.N. contributed to preparing the manuscript. N.A., M.S., and S.A. Rao helped with manuscript writing.

Data availability The gridded data used in this study can be obtained from the IMD website (imdpune.gov.in). Any other data may be made available from the corresponding author at a reasonable request.

Declarations

Competing interests The authors declare no competing interests.

Conflict of interest The authors have no conflicts of interest in this work.

References

- Baño-Medina J, Manzanas R, Gutiérrez JM (2020) Configuration and intercomparison of deep learning neural models for statistical downscaling. *Geosci Model Dev* 13:2109–2124. <https://doi.org/10.5194/gmd-13-2109-2020>
- Cheng J, Kuang Q, Shen C, Liu J, Tan X, Liu W (2020) ResLap: generating high-resolution climate prediction through image super-resolution. *IEEE Access* 8:39623–39634. <https://doi.org/10.1109/ACCESS.2020.2974785>
- Dong C, Loy CC, He K, Tang X (2015) Image super-resolution using deep convolutional networks. *CoRR* abs/1501.00092
- Dueben PD, Bauer P (2018) Challenges and design choices for global weather and climate models based on machine learning. *Geosci Model Dev* 11:3999–4009. <https://doi.org/10.5194/gmd-11-3999-2018>
- Gagne DJ, Christensen HM, Subramanian AC, Monahan AH (2020) Machine learning for stochastic parameterization: generative adversarial networks in the Lorenz '96 Model. *J Adv Model Earth Syst* 12:e2019MS001896. <https://doi.org/10.1029/2019MS001896>
- Goodfellow IJ, Pouget-Abadie J, Mirza M, Xu B, Warde-Farley D, Ozair S, Courville A, Bengio Y (2014) Generative adversarial nets. In: Proceedings of the 27th international conference on neural information processing systems. MIT Press, Cambridge, pp 2
- Haq MA (2022a) CDLSTM: a novel model for climate change forecasting. *Comput Mater Contin* 71:2363–2381. <https://doi.org/10.32604/cmc.2022.023059>
- Haq MA (2022b) SMOTEDNN: a novel model for air pollution forecasting and AQI classification. *Comput Mater Contin* 71:1403–1425. <https://doi.org/10.32604/cmc.2022.021968>
- Haq MA, Khan MAR (2022) DNNBoT: deep neural network-based botnet detection and classification. *Comput Mater Contin* 71:1729–1750. <https://doi.org/10.32604/cmc.2022.020938>
- Haq MA, Azam MF, Vincent C (2021) Efficiency of artificial neural networks for glacier ice-thickness estimation: a case study in western Himalaya, India. *J Glaciol* 67:671–684. <https://doi.org/10.1017/jog.2021.19>
- Haq MA, Khan MAR, AL-Harbi T (2022) Development of PCCNN-based network intrusion detection system for EDGE computing. *Comput Mater Contin* 71:1769–1788. <https://doi.org/10.32604/cmc.2022.018708>
- Harilal N, Singh M, Bhatia U (2021) Augmented convolutional LSTMs for generation of high-resolution climate change projections. *IEEE Xplore* 9:25208–25218. <https://doi.org/10.1109/ACCESS.2021.3057500>
- Harris L, McRae ATT, Chantry M, Dueben PD, Palmer TN (2022) A generative deep learning approach to stochastic downscaling of precipitation forecasts. *J Adv Model Earth Syst* 14:e2022MS003120. <https://doi.org/10.1029/2022MS003120>
- Izumi T, Amagasaki M, Ishida K, Kiyama M (2022) Super-resolution of sea surface temperature with convolutional neural network- and generative adversarial network-based methods. *J Water Clim Chang* 13:1673–1683. <https://doi.org/10.2166/wcc.2022.291>
- Kumar B, Chattopadhyay R, Singh M, Chaudhari N, Kodari K, Barve A (2021) Deep learning-based downscaling of summer monsoon rainfall data over Indian region. *Theoret Appl Climatol* 143:1145–1156. <https://doi.org/10.1007/s00704-020-03489-6>
- Kumar B, Abhishek N, Chattopadhyay R, George S, Singh BB, Samanta A, Patnaik BSV, Gill SS, Nanjundiah RS, Singh M (2022) Deep learning based short-range forecasting of Indian

- summer monsoon rainfall using earth observation and ground station datasets. *Geocarto Int*:1–28. <https://doi.org/10.1080/10106049.2022.2136262>
- Ledig C, Theis L, Huszar F, Caballero J, Cunningham A, Acosta A, Aitken A, Tejani A, Totz J, Wang Z, Shi W (2017) Photo-realistic single image super-resolution using a generative adversarial network. arXiv.org
- Leinonen J, Guillaume A, Yuan T (2019) Reconstruction of cloud vertical structure with a generative adversarial network. *Geophys Res Lett* 46:7035–7044. <https://doi.org/10.1029/2019GL082532>
- Leinonen J, Nerini D, Berne A (2020) Stochastic super-resolution for downscaling time-evolving atmospheric fields with a generative adversarial network. arXiv.org. <https://doi.org/10.1109/TGRS.2020.3032790>
- Liu J, Sun Y, Ren K, Zhao Y, Deng K, Wang L (2022) A Spatial downscaling approach for windsat satellite sea surface wind based on generative adversarial networks and dual learning scheme. *Remote Sensing* 14. <https://doi.org/10.3390/rs14030769>
- Oliver MA, Webster R (1990) Kriging: a method of interpolation for geographical information systems. *Int J Geogr Inf Syst* 4:313–332. <https://doi.org/10.1080/02693799008941549>
- Oyama N, Ishizaki NN, Koide S, Yoshida H (2022) Deep generative model super-resolves spatially correlated multiregional climate data. <https://doi.org/10.48550/arXiv.2209.12433>
- Pai DS, Stidhar L, Rajeevan M, Sreejith OP, Satbhai NS, Mukhopadhyay B (2014) Development of a new high spatial resolution (0.25°). *Passarella LS, Mahajan S, Pal A, Norman MR (2022) Reconstructing high resolution ESM data through a novel Fast Super Resolution Convolutional Neural Network (FSRCNN). Geophys Res Lett 49:e2021GL097571. https://doi.org/10.1029/2021GL097571*
- Rajeevan M, Bhate J, Kale JD, Lal B (2006) High resolution daily gridded rainfall data for the Indian region: analysis of break and active monsoon spells. *Curr Sci Assoc* 91:296–306
- Reichstein M, Camps-Valls G, Stevens B, Jung M, Denzler J, Carvalhais N, Prabhat (2019) Deep learning and process understanding for data-driven Earth system science. *Nature* 566:195–204. <https://doi.org/10.1038/s41586-019-0912-1>
- Sanjay J, Ramarao MVS, Ingle S, Singh BB, Krishnan R (2020) Regional climate change datasets for South Asia. *axiv* 1–4. <https://doi.org/10.48550/arXiv.2012.10387>
- Seaby LP, Refsgaard JC, Sonnenborg TO, Stisen S, Christensen JH, Jensen KH (2013) Assessment of robustness and significance of climate change signals for an ensemble of distribution-based scaled climate projections. *J Hydrol* 486:479–493. <https://doi.org/10.1016/j.jhydrol.2013.02.015>
- Serifi A, Günther T, Ban N (2021) Spatio-temporal downscaling of climate data using convolutional and error-predicting neural networks. *Front Climate* (3):1–15. <https://doi.org/10.3389/fclim.2021.656479>
- Simonyan K, Zisserman A (2015) Very deep convolutional networks for large-scale image recognition. arXiv:1409.1556. <https://doi.org/10.48550/arXiv.1409.1556>
- Singh BB, Singh M, Singh D (2021) An overview of climate change over South Asia: observations, projections, and recent advances. In: Singh RB, Chatterjee S, Mishra M, de Lucena AJ (Eds.), *Practices in regional science and sustainable regional development: experiences from the global south*. Springer Singapore, Singapore, pp. 263–277. https://doi.org/10.1007/978-981-16-2221-2_12
- Stengel K, Glaws A, Hettinger D, King RN (2020) Adversarial super-resolution of climatological wind and solar data. *Proc Nat Acad Sci* 117:16805–16815. <https://doi.org/10.1073/pnas.1918964117>
- Vandal T, Kodra E, Ganguly S, Michaelis A, Nemani R, Ganguly AR (2017) DeepSD: Generating high resolution climate change projections through single image super-resolution. arXiv.org 1–9. <https://arxiv.org/abs/1703.03126>
- Xiong Y, Guo S, Chen J, Deng X, Sun L, Zheng X, Xu W (2020) Improved SRGAN for Remote Sensing Image Super-Resolution Across Locations and Sensors. *Remote Sensing* 12(8):1263. <https://doi.org/10.3390/1263rs1208>

Publisher's note Springer Nature remains neutral with regard to jurisdictional claims in published maps and institutional affiliations.

Springer Nature or its licensor (e.g. a society or other partner) holds exclusive rights to this article under a publishing agreement with the author(s) or other rightsholder(s); author self-archiving of the accepted manuscript version of this article is solely governed by the terms of such publishing agreement and applicable law.